Binary phase diagrams of H_2-He mixtures at high temperature and high pressure

P. Loubeyre, R. Le Toullec, and J. P. Pinceaux
Physique des Milieux Condenses, Tour 13, E4, Université Pierre et Marie Curie, 4 place Jussieu, Paris 75252, France
(Received 24 July 1986; revised manuscript received 24 February 1987)

The binary phase diagrams of H_2-He mixtures have been measured up to 373 K and 10 GPa in a diamond-anvil cell. The measurements of the visualized phase transitions in mixtures of known initial concentrations were completed by the Raman measurements of the shift of the Q_1 vibron of H_2 molecules, calibrated as a gauge of the concentrations of the separated phases. Evolution of singularities of the demixing diagram indicates that the two-fluid domain may close up and separate from the solid-fluid region at higher pressures and temperatures.

I. INTRODUCTION

H_2 and He stand out among the elements due to their molecular and atomic simplicities. This makes their properties most amenable to a theoretical treatment based on first principles. They also seem to be interesting candidates for extraordinary phenomena such as the superconductivity of metallic hydrogen at high temperature.[1] Measurements of their high-pressure phase diagrams[2,3] have sensitively tested the interactions and the models which were used in their theoretical analyses. Furthermore, the Raman shift of the Q_1 vibron of the H_2 molecule under pressure[4] follows the evolution of the intramolecular bonding prior to the metallization of solid H_2. Then, the present study of H_2-He mixtures could be a test of mixture theories at very high density since the interactions of such systems are now well known. In addition to this fundamental aspect, H_2 and He are the main constituents of our solar system and better knowledge of their condensed phases, especially their miscibility, is needed to improve models of the Jovian planets.

Studies on mixtures at high pressures with a diamond-anvil cell (DAC) are in a primitive state since they are somewhat more complex than measurements on one-component systems. This can be illustrated by listing a few of the difficulties encountered in the present study, as regards both implementation and analysis of experiments:

(i) H_2 and He have different liquefaction points at ambient pressure which prevents cryogenic loading of the cell. A specific setup, which is described below, had to be used.

(ii) Hydrogen embrittlement and the explosive nature of H_2-air mixtures require special experimental care and use of hydrogen-resistant alloys.

(iii) The usual measurements of *in situ* concentrations cannot be used in the DAC; this was solved by using the Q_1 vibron of the H_2 molecule[5] which we calibrated and used as a concentration gauge of the separated phases.

(iv) Also theoretically, the He molar concentration of the mixture, denoted x in the following, is added as a third dimension to the usual (P,T) phase diagram of a pure element; it increases the complexity of the analysis of the phase diagram which is illustrated by going from a melting point for a one-component system to the isothermal binary phase diagram as shown in Fig. 1(a).

The binary phase diagrams of H_2-He mixtures have been previously studied by Streett[6] up to $P=1$ GPa and $T=100$ K in the range of classical high-pressure bombs. Recently, Schouten *et al.*[7] have extended this investigation to higher pressures: They measured, up to 5 GPa in a DAC, the pressures where fluid-fluid and solid-fluid separations of phases occur, as a function of temperature, for a mixture of initial helium concentration $x=0.58$; from this they concluded that the extent of the fluid-fluid demixing domain increases with density.

In the present study we report isothermal binary phase diagrams at $T=295$ and 373 K. In the following it will be clear that their detailed shapes had to be investigated in order to reach the conclusion that the fluid-fluid domain may close up at higher temperatures. In Sec. II, the experimental setup is briefly described, mainly to stress some of its novel features. In Sec. III we explain the methods used to construct the phase diagrams. In Sec. IV our results at ambient and high temperatures are discussed.

II. EXPERIMENTAL SETUP

Two techniques allow loading a diamond-anvil cell with gas: In cryogenic methods the cell is cooled below the liquefaction point of the gas and then sealed when the gasket hole is loaded with liquid. An alternative is high-pressure room-temperature loading in a vessel containing the DAC which is then closed *in situ*, trapping the sample at a sufficient density. The cryogenic setup was mostly used for DAC studies of pure components but cannot be used for mixtures, since, as a rule, the liquefied gases are not miscible at all concentrations.

The diamond-anvil cell built for this study is an improvement over that which was used for the study of He;[8] it will be described more fully in a planned forthcoming paper[9] and we briefly present here only its main characteristics which are relevant to this work: It is made out of beryllium copper (Be-Cu), which is not susceptible to hydrogen embrittlement. The body is a cylinder, 50 mm in height and in outside diameter. An improvement of this setup is that the force on the diamonds is generated by a low-pressure gas (1–30 MPa), driving a flexible metal

membrane acting as a bellows. Small variations of pressure can thus be generated and this sensitivity has made possible the investigation of the binary phase diagram at constant temperature. Microscope objectives give optical access to both sides of the cell: One focuses a 10-μm laser spot onto the sample, and the other is used to collect scattered light which is analyzed in a spectrometer. The sample space initially is a cylinder limited by the two culets of the diamonds and a hole in a Be-Cu gasket, 150 μm in diameter and some 50 μm thick; a thermocouple is soldered on the Be-Cu gasket to measure the temperature of the sample with a precision of about 0.5 K. The filling procedure is as follows: The gas mixture is prepared at 15 MPa and the concentration taken to be the ratio of the partial pressures. The gas is then compressed to 150 MPa at room temperature in the pressure vessel containing the diamond-anvil cell. The diamonds are then pressed into a Be-Cu gasket by exerting an adequate overpressure on the membrane, and the setup is then depressurized down to room pressure while maintaining the sample sealed off in the cell. The samples are then typically 100 μm in diameter and 30 μm thick. All the parts in the setup are compatible with hydrogen. The pressure was measured by the ruby-luminescence scale with a pressure coefficient of -7.57 cm^{-1}GPa and a temperature coefficient of -0.14 cm^{-1}/K.[10] The DAC is put in an adapted thermostat where the selected temperature could be maintained with temperature variations less than 0.2 K. The microscope objectives are Leitz U.M.32 with a 14-mm frontal distance. They are used either to directly observe the phase transitions of the sample or to focus the beam of the 488-nm line of an Ar^+ laser on the sample and collect the Raman signal in the forward-scattering geometry. The Q_1 vibrational mode of the H_2 molecule was measured in a triple 2.4-m monochromator (T800 Coderg). The power of the laser beam on the sample was kept lower than 300 mW. Heating of the medium was investigated by varying the power of the laser beam by at least a factor of 2: no change could be detected either on the location of the phase transitions or on the concentrations of the separated phases (if a thermal effect were present, it would have modified the concentrations of the separated phases in equilibrium and, consequently, as shown below, this would have been reflected by the Raman frequency of the Q_1 vibronic mode of H_2). The insensitivity of the system to comparatively high power densities is related to the transparency of H_2-He mixtures in the visible and excellent thermal conductivity of the diamond anvils.

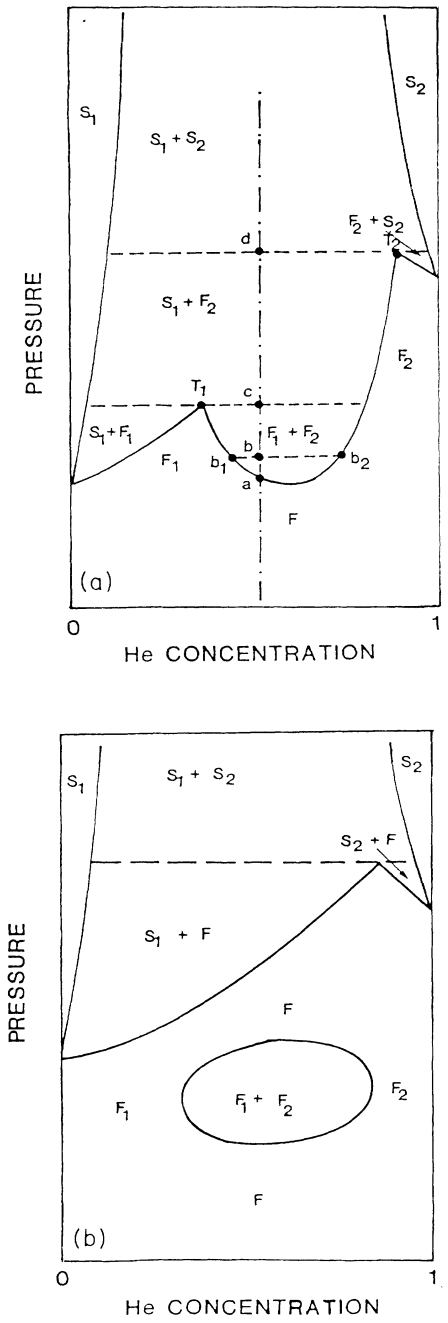

FIG. 1. Two types of isothermal binary phase diagrams: (a) The most usual shape similar to the low-temperature H_2-He diagrams. The dashed-dotted line indicates the different phases of the evolution of a mixture of initial concentration x with pressure. (b) Presenting a closed fluid-fluid separation domain.

Two ways of probing the binary phase diagram, either by direct observation of phase transitions for different initial helium concentrations or by inversion of the Raman measurements of the Q_1 mode of H_2 with the $S(x)$ function, were used as complementary methods to construct its detailed shape, as shown in the next section.

III. CONSTRUCTION OF THE PHASE DIAGRAM

A. Direct visualization measurements

The thermodynamics of a binary phase diagram is governed by three independent parameters: the pressure P, the temperature T, and the molar concentration x of one component, helium in the present study. Phase boundaries in this three-dimensional phase diagram are surfaces given by the loci of the (P,T,x) points for which the thermodynamical potentials of two phases are

equal. Such a diagram is usually constructed by studying its two-dimensional sections, in which case the phase boundaries show as transition lines; this is obtained by setting the temperature or the pressure constant. For the present study isothermal sections are shown since, as explained above, the membrane device allows quite sensitive pressure variations under controlled temperature. We are now going to describe the main characteristics of such an isothermal binary phase diagram, which may help in the following analyses of our measurements. A more detailed description of the subtleties of H_2-He binary phase diagrams may be found in Ref. 6.

A sketch of the main features of an isothermal binary phase diagram is shown in Fig. 1(a): solid lines enclose thermodynamical states were the system separates into two phases (or three at triple points T_1 or T_2). The thermodynamical states of the separated phases are given by the intersection of the horizontal isobar, going through the point representing the state of the system, with the boundary lines, as shown on state b, which separates into fluids F_1 of state b_1 and F_2 of state b_2.

In Fig. 1(b) is shown a speculative binary phase diagram which will be discussed in the conclusion as a possibility for H_2-He mixtures at high density.

A straightforward method of constructing isothermal binary phase diagrams at high pressure in DAC experiments is to measure the pressure at which the phase transitions are visually detected for different initial concentrations. As an illustration, we will describe the isothermal evolution of a mixture of initial molar concentration of helium, x, with pressure; that is, following the vertical dashed and dotted line in Fig. 1(a): At point a, the homogeneous fluid mixture separates into a small bubble of He-rich fluid F_2, surrounded by H_2-rich fluid F_1. When the pressure is raised the volume of the F_2 bubble increases up to point c, where there is an equilibrium between three phases: solid S_1, fluid F_1, and fluid F_2; between c and d there is an equilibrium between solid S_1, which is easily identified by its granulation and shape, and fluid F_2; above d, the solid-solid demixing brings about a mixture of polycrystals with numerous grain boundaries. The relative amounts of the two phases are given by the lever rule; for example, at point b the ratio of the mole fractions of phase b_1 to phase b_2 is equal to the inverse ratio of the absolute values of the differences between the He molar volume at phase b with those at the separated phases, b_1 and b_2; this is why, at point a, only a small bubble of fluid F_2 appears, which then increases with pressure.

The whole isothermal binary phase diagram can be obtained by interpolation between similar measurements of points a, for various initial helium concentrations. Such points are shown as asterisks in Fig. 2. Points c and d give the pressures of the triple points T_1 and T_2. These direct measurements were complemented by indirect ones obtained from the Raman shift of the Q_1 vibron mode of H_2 molecules.

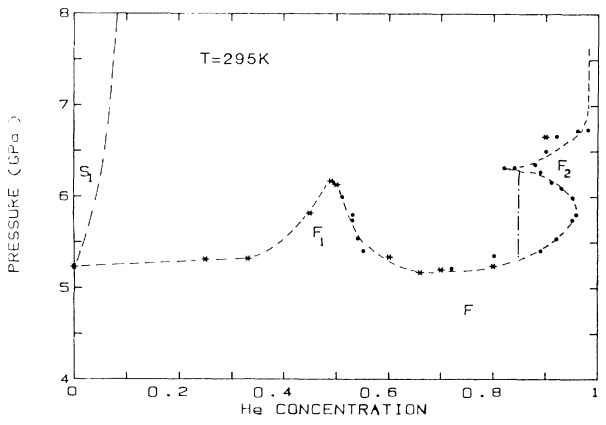

FIG. 2. The isothermal binary phase diagram of H_2-He mixtures at 295 K. The asterisks mark the direct visualization measurements; the dots mark the indirect ones obtained from the inversion of the Raman-shift measurements by the $S(x)$ function. At the right of the vertical dashed-dotted line metastable behavior could be obtained.

B. Raman concentration gauge

A remarkable feature of the Raman shift of the Q_1 vibronic mode of the H_2 molecule with pressure is its strong dependence on He concentration at a given pressure: the

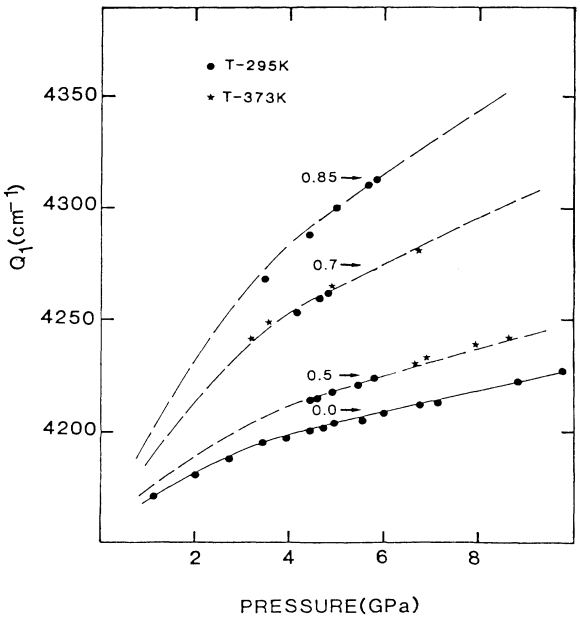

FIG. 3. Evolution of the Raman frequency of the Q_1 vibronic mode of H_2 with pressure in homogeneous fluid mixtures of initial He concentrations: 0.0 (pure H_2), 0.5, 0.7, and 0.85. The dots mark the measurements at $T=295$ K and the asterisks those at 373 K. The solid line is the fit of the measurements of Ref. 4; the dashed lines are obtained from this fit by the multiplicative constant, $S(x)$, which gauges the increased shift in a mixture of He concentration x at the same pressure. The (small) negative jump of the H_2 curve at solidification (5.3 GPa) has been smoothed out.

richer in helium the surrounding medium is, the larger the shift is. We have reported this effect in a previous article and explained it semiquantitatively in terms of a helium compressional effect.[5] We have quantified it by the $S(x)$ function

$$S(x)=[Q_1(x,P)-Q_1(0,0)]/[Q_1(0,P)-Q_1(0,0)] ,$$

where $Q_1(x,P)$ is the Raman frequency of the Q_1 vibronic mode of H_2 in a mixture of helium concentration x and at pressure P; $Q_1(0,0)$ is the frequency of the isolated molecule equal to 4155.2 cm^{-1}. $S(x)$ was found to be independent of pressure in the range investigated, as shown in Fig. 3. In this figure the observed Raman frequencies of several homogeneous fluid mixtures versus pressure, at $T=295$ and 373 K, are shown and compared with the $x=0$ (pure hydrogen) dependence. The point here, that $S(x)$ is independent of pressure, just means that the observed Raman frequencies for a given concentration lie on lines which are derived from the pure H_2 curve by a constant pressure-independent factor: these curves (plotted as dashed lines) do indeed fit with our observations, at least in the range of interest; that is, above 4 GPa.

$S(x)$ is plotted in Fig. 4, where the asterisks denote the concentrations where it has been calibrated. It is clear that $S(x)$, or more rigorously its inverse function, can be used as a convenient gauge of the He concentrations larger than 0.45, but is of little use in the low-concentration region.

In Fig. 5 we have plotted the full width at half maximum height Ω of the Q_1 Raman peak as a function of helium concentration in the homogeneous fluid phase; it strongly increases with x, which is a consequence of inhomogeneous broadening due to the statistical distribution of local environment patterns of a given molecule.[11] As the average He concentration x increases, a change in the local environment of an H_2 molecule, which is equivalent to a local fluctuation of x, will induce a large variation in the shift when $dS(x)/dx$ is large at the equilibrium concentration. Thus this half-width dependence is directly related to the first derivative of $S(x)$, as can be seen by comparing Figs. 4 and 5. Therefore, Raman measurements were difficult in the He-rich phases since as x increases the peak broadens and its integrated intensity, which is proportional to x, decreases: both effects contribute to decreasing the signal maximum.

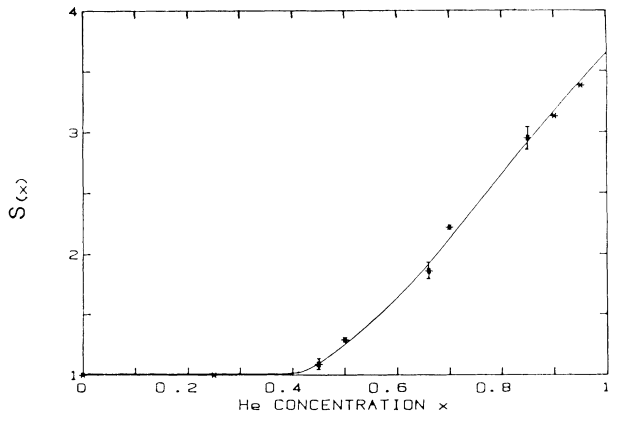

FIG. 4. Ratio $S(x)$ of the Raman shift, induced by the pressure, of the Q_1 mode in a fluid mixture of He concentration x over that in pure H_2, vs x. The asterisks are measurements and the solid line interpolates between them.

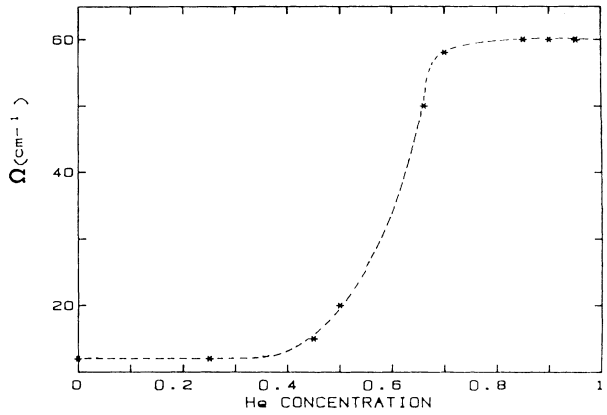

FIG. 5. Full width at half maximum height, $\Omega(x)$, of the Raman peak of the Q_1 mode in homogeneous fluid mixtures of He concentrations x. The asterisks are the measurements and the dashed line interpolates between them.

In constructing the $S(x)$ function, the Q_1-mode frequency in pure H_2 plays a reference role. We have therefore carefully checked the measurements of Sharma *et al.*[4] against ours up to 15 GPa to eliminate a possible difference in the spectrometer calibration. The agreement with their results is better than our error bars, estimated to be 1 cm^{-1} as seen in Fig. 3, in which the solid line is their analytical fit and the dots some of our measurements; we have used this fit to construct $S(x)$.

IV. RESULTS

A. Variation of the Raman frequency with pressure at 295 K

Depending on the initial concentration of the mixture, three different trends have been observed, which are illustrated at room temperature in Figs. 6 and 7.

(i) For $x<0.5$ (Fig. 6), the homogeneous fluid separates into fluid F_1 and solid S_1. The solid being almost pure H_2, its vibron frequencies are very close to those of the H_2 solid. Note that for the concentrations shown in Fig. 6, $x=0.25$ and 0.45, the upper F_1 branch of the diagram follows the F_1 demixing curve on the left of triple point T_1 [Fig. 1(a)], and therefore terminates at 6.2 GPa, which is the pressure of the triple point T_1 at 295 K, drawn in Fig. 6 as a square.

(ii) For concentrations higher than 0.5 and up to 0.8, the dependence of Q_1 versus pressure is shown in Fig. 7. Demixing first occurs between fluids F_2 and F_1, the latter ending at point T_1, drawn as a square, where separation S_1+F_2 starts. A common feature for all concentrations

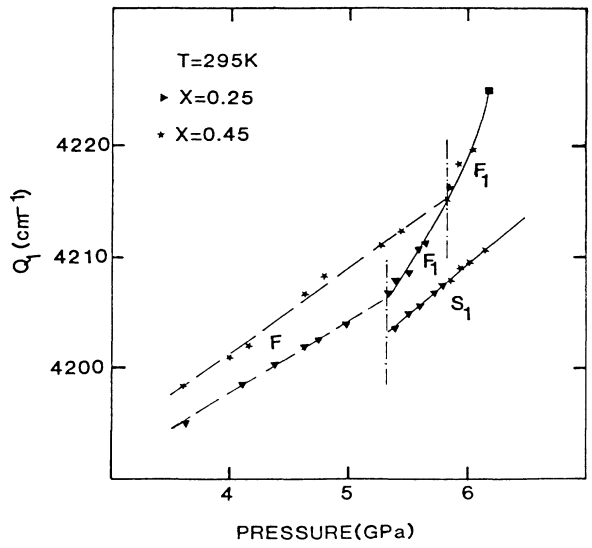

FIG. 6. Evolution of the Raman frequency of the vibronic Q_1 mode in mixtures of initial He concentrations $x=0.25$, marked by triangles, and $x=0.45$, marked by asterisks, at $T=295$ K. The dashed-dotted lines indicate the transition from the homogeneous fluid to the separation of phases F_1+S_1. The solid lines are the loci of the equilibrium states of the separation of phases at a given pressure; the F_1 line ends at the triple point T_1 marked by a square.

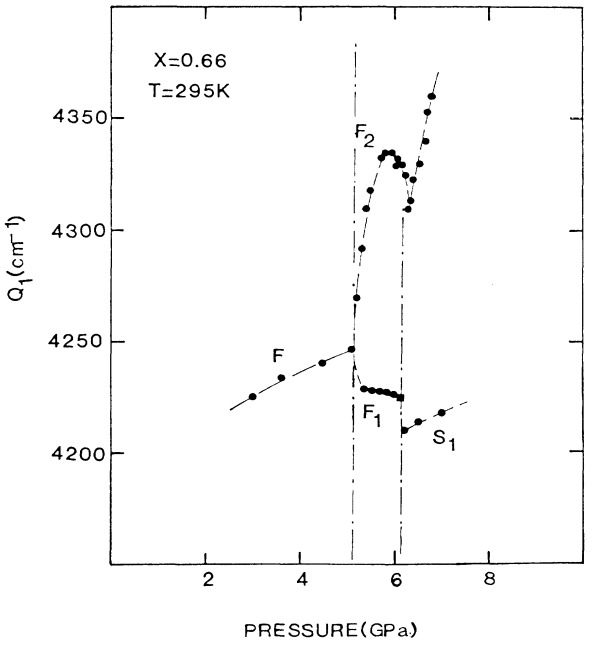

FIG. 7. Evolution with pressure of the Raman frequency of the vibronic Q_1 mode of H_2 in a mixture of initial He concentration $x=0.66$ at $T=295$ K. The dashed-dotted lines indicate the transition from the homogeneous fluid to the fluid-fluid separation F_1+F_2 and from it to the solid-fluid separation F_2+S_1. The F_1 line ends at the triple point T_1 marked by a square. The dashed lines interpolate between experimental points (dots).

above $x=0.5$ is the singularity at 6.3 GPa on the F_2 branch, which is not to be related to the F_1-S_1 transition (lower branch) which occurs 0.1 GPa lower, at room temperature: Indeed, as we shall see in the next paragraph, this cusp on the F_2 curve occurs 0.6 GPa lower than the F_1-S_1 transition, at 373 K.

(iii) Mixtures with concentrations $x=0.85$ or 0.90 behaved, on occasion, rather differently: upon increase of pressure we do not observe an F_1+F_2 separation of phases. In fact, it means that we can metastably keep a homogeneous He-rich fluid up to pressures where it should be separated. The same metastable behavior could also be obtained in decreasing the pressure from the F_2+S_1 separation of phases; in this case the F_2 fluid phase would follow the vertical dashed-dotted metastable line in Fig. 2 instead of the equilibrium one.

In the three cases, for pressures above the triple point T_2 (roughly given by $x=0.98$ and $P=12$ GPa), there is a separation between two solids, not reported here since we could not measure the Q_1 Raman shift in S_2. It should also be noted that the areas of the separated phases had to be larger than the laser spot so that the Raman measurement could be done. This point, together with the lever rule, explains why there is a maximum pressure above which the shift of the Q_1 mode in the F_1 phase is not reported on the $x=0.25$ example of Fig. 6. When the volume areas of the separated phases were large enough, no parasitic influence of laser heating could be detected as pointed out above.

B. Construction of the binary phase diagram at room temperature

Once the $S(x)$ helium concentration gauge has been calibrated, construction of the boundary lines of the F_1+F_2 domain is straightforward from the inversion of the measurements of the Raman shift of the Q_1 mode in both separated fluid phases. Apart from the 0.66 concentration illustrated in Fig. 7, other initial concentrations (0.7, 0.75) were studied and exhibit the same Q_1-versus-P behavior in the separation region since the equilibrium thermodynamical states of their separated phases are all the same at a given pressure; the Raman data are then converted into concentrations by the inverse function of $S(x)$ and these two curves give, in the separation region, the concentrations of the F_1 and F_2 phases in equilibrium as a function of pressure P, which are the boundary lines of the F_1+F_2 domain in the binary phase diagram; they are plotted as dots in Fig. 2. This diagram has the global shape of Fig. 1(a), but its details are worth a closer analysis.

(a) The concentration of the critical point ($dP/dx=0$) has moved from 0.58 at low temperature to 0.68 at 295 K and the concentration of the triple point T_1 from less than 0.2 to 0.49. These two facts indicate an increasing mutual solubility of H_2-He mixtures with temperature.

(b) Most interestingly, the boundary line between the F_1+F_2 domain and the homogeneous F_2 fluid region has a peak. Such a feature could point to the evolution of the F_1+F_2 domain towards it closing up by an upper critical point as represented in Fig. 1(b). The metastable behavior

is probably related to this, but an understanding of its microscopic mechanism is unclear.

Furthermore, it is easily seen from Fig. 2 that the binary phase diagram which could have been constructed from the interpolation between direct visualization measurements, i.e., interpolated between the asterisks, would have missed the interesting cusp point; the metastable behavior of the He-rich fluid mixtures alters such a construction. It thus clearly evidences that both methods of investigation, the direct visualization and the Raman measurements of the Q_1 mode, were needed for the construction of the detailed binary phase diagram. Indeed, the latter method is sufficient using only a few initial concentrations to probe all the demixing diagram at the right of the triple T_1 point.

Two important qualitative properties of the H_2-He mixtures were observed during the room-temperature measurements: First, we noted that in the fluid-fluid demixing regime the He-rich fluid formed a bubble surrounded by the H_2-rich fluid, independently of their volume ratio; consequently, this means that the surface tension is larger in the He-rich fluid than in the H_2-rich one. Second, we observed an inversion of density between the He-rich fluid phase and the H_2-rich one at a pressure of 5.24 GPa: From this we infer that, at 5.24 GPa, the density of the fluid is the same for $x=0.6$ and 0.8, since they are the two He concentrations in equilibrium at $P=5.24$ GPa (Fig. 2). This density inversion was directly observed since we could move around the He-rich fluid bubble in the cell with the laser beam and observe its motion in the gravitational field. For an ideal mixture, the fluid phase the richer in He should be the denser; this effect is thus related to the excess volume of mixing.

C. Binary phase diagram at 373 K

Going to higher temperatures will test the trend of the fluid-fluid domain to close up, as suggested from the shape of the isothermal binary phase diagram at $T=295$ K. Therefore the DAC was put in a thermostat and at high temperature the procedure for exploring the binary phase diagram was the same as described in the preceding section. In Fig. 3 we have also shown the evolution of the Raman shift of the vibron Q_1 in homogeneous fluid mixtures for helium concentrations $x=0.5$ and 0.7 at $T=373$ K (asterisks) and compared them with $T=295$ K (dots): It is clear that the influence of this change of temperature on the Raman shift is very small and our concentration gauge $S(x)$, calibrated at 295 K, is still accurate enough at 373 K.

Before presenting our high-temperature measurements, we note an experimental feature which has appeared at high temperature and presented a serious drawback: H_2 diffusion into the Be-Cu gasket took place at $T=373$ K; this appears only in mixtures very rich in He and this disadvantageous effect had to be reduced by a thermal treatment of the gasket. This effect is pointed out mainly to show the high-temperature limit of the present experimental investigation. The following results were obtained by a number of loadings of the cell and carefully checked. In Fig. 8 the Raman shift of the Q_1 mode was measured

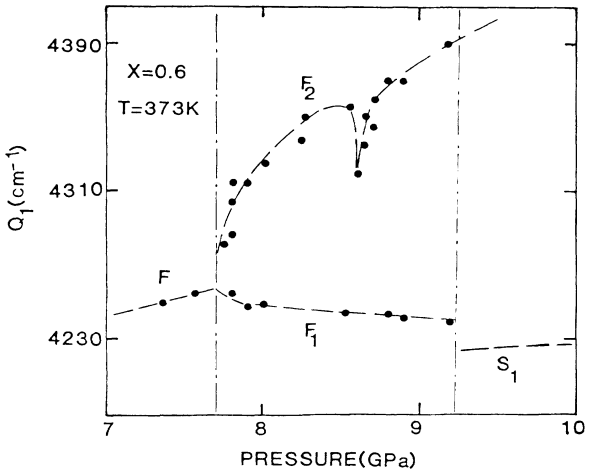

FIG. 8. Evolution with pressure of the Raman frequency of the vibronic Q_1 mode of H_2 in a mixture of initial He concentration $x=0.6$ at $T=373$ K.

at $T=373$ K in the separated fluid phases of an homogeneous fluid mixture of initial concentration $x=0.6$. As for $T=295$ K, such measurements were confirmed for other initial concentrations (x=0.66, 0.75). Inverting these results with the $S(x)$ gauge gives the boundaries of the F_1+F_2 domain of the $T=373$ K binary phase diagram. These data are compared in Fig. 9 to the results at $T=295$ and 100 K of Ref. 6.

Two features can be pointed out.

(i) As noted by Streett[6] from his measurements up to 100 K and confirmed by Schouten at higher temperatures,[7] the pressure difference between the critical point and the triple point T_1 increases with the temperature. From this, we can only conclude that the extension of the P-T domain of the fluid-fluid region will not be limited at

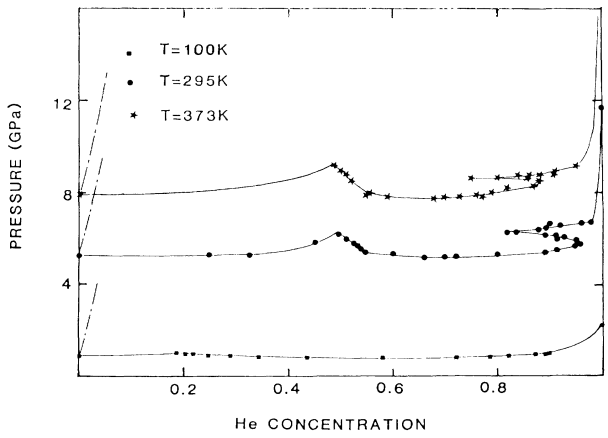

FIG. 9. Isothermal binary phase diagrams of H_2-He mixtures at $T=100$ (squares), 295 (dots), and 373 K (asterisks). The solid lines interpolate between the experimental points; the dashed-dotted lines show the hypothetical S_1 domains.

higher densities by the pressure-induced solidification of the less volatile component, here H_2, as observed in the case of Ar-He mixtures.[12]

(ii) This set of data confirms the structure of the F_1+F_2 domain which has a peak on its transition line with F_2. This effect is even more apparent at $T=373$ K. We interpret this as the intermediate stage of the evolution of the fluid-fluid domain towards its closing up at higher densities; that is, going from the situation of Fig. 1(a) to that of Fig. 1(b). If this is the case, from Fig. 9 we can roughly estimate the upper critical endpoint above which the F_1+F_2 domain should close up: it is given by the intersection of the line joining the loci of the triple T_1 points at $T=295$ and 373 K and that joining the two cusp points, which gives a pressure around 20 GPa [which corresponds by extrapolation of the (P,T) loci of the T_1 triple point to a temperature in the range 600–800 K]. Above this point ($P=20$ GPa, $T=600$–800 K) the fluid-fluid domain in the isobar or isotherm cuts may have the shape of Fig. 1(b). The x position of the triple T_1 point cannot be extrapolated in a simple manner from the data of Streett[6] up to 100 K and 1 GPa which, for T_1, would give $x=0.28$ at 295 K and $x=0.3$ at 373 K. The reasons for this could be the influence of quantum effects which, at low temperature, are roughly twice as large in H_2 than in He and greatly modify the thermodynamics of the system; or, noting that the He concentration of T_1 is equal to 0.5 ± 0.2 and does not vary between 295 and 373 K within experimental error, it could indicate the relative stabilization with density of the fluid equally composed of He atoms and H_2 molecules ($x=0.5$).

V. CONCLUSION

Detailed isothermal binary phase diagrams of H_2-He mixtures at high densities can therefore be obtained in the DAC by making use of an *ad hoc* concentration gauge; that is, the calibration of the influence of the He concentration on the Raman shift of the Q_1 mode of H_2 molecules with pressure. To our knowledge, the present data are the first experimental observation of a fluid-fluid domain exhibiting such a peak shape on the transition line between the F_1+F_2 and F_2 regions. This points to its evolution with density towards a closed domain and a very rough extrapolation predicts the existence of an upper critical endpoint in the vicinity of 20 GPa and 600–800 K. Although the measurements of such a point are now within experimental reach, the present device would have to be modified in order to maintain a temperature of the order of 800 K. Adequate gasket material would have to be used in order to prevent H_2 diffusion at high temperatures. Checking this speculation of a closed F_1+F_2 domain is in order and work in this direction is in progress in our laboratory.

The present measurements should also be useful for testing mixtures theories and for our understanding of Jovian planets.

(i) Fluid theories of mixtures seem to be quite accurate now and, for example, Ree[13]—with a van der Waals—type theory of mixtures—could reproduce the results of Streett on the low-temperature binary phase diagram of H_2-He mixtures. However, such calculations might not be reliable and accurate enough at high densities to reproduce the observed peak structure on the F_1+F_2 boundary line.

(ii) Since the study of such systems was first initiated by astrophysicists, it seems reasonable to conclude with a remark about possible consequences of these measurements on the models of the interior of Jovian planets: their He concentration being less than 0.5 (for Saturn it is supposed to be 0.35), there should be no fluid-fluid separation of phases. However, if at a given depth higher concentrations of He exist, there will be a layer of separated fluid-fluid phases which could be of some influence on the convection modes and the energy flow of the planet.

We are not able to pursue this field further and leave these questions to astrophysicists as an example of interaction between high-pressure research in physics and planetary-interior modeling.

Note added. Van den Bergh *et al.* have recently published measurements of the H_2-He binary phase diagrams up to 75 kbar [Physica **141A**, 524 (1987)]. Their He-concentration measurements are in strong disagreement with those of the present work; for example, the He concentration of their triple point T_1 is 0.23, but in the present work it is 0.49 at 295 K. The main source of error in such experiments is H_2 diffusion during the loading of the cell and in the gasket. If such an effect were taking place, it would give a measured binary phase diagram in which the transition lines are systematically shifted to the low-He-concentration region. This thus tends to give credibility to the present work. Furthermore, the details of the binary phase diagrams could only be obtained with the use of the Raman concentration gauge as demonstrated in the present work.

ACKNOWLEDGMENTS

We thank J. M. Besson for continuous interest in this work, many helpful discussions, and a careful reading of the manuscript. This work was supported in part by the Commissariat a l'Energie Atomique under Grant No. C1880P1A and by the Institut National d'Astronomie et de Geophysique under Grant No. 83070978. The Physique des milieux condenses is an equipe associeé au Centre National de Recherches Scientifiques (UA 782).

[1] N. W. Ashcroft, Phys. Rev. Lett. **21**, 1748 (1968).

[2] I. F. Silvera, Rev. Mod. Phys. **52**, 393 (1980).

[3] P. Loubeyre, J. M. Besson, J. P. Pinceaux, and J. P. Hansen, Phys. Rev. Lett. **49**, 1172 (1982); P. Loubeyre, Physica **139&140B**, 224 (1986).

[4] S. K. Sharma, H. K. Mao, and P. M. Bell, Phys. Rev. Lett. **44**, 886 (1980).

[5] P. Loubeyre, R. Le Toullec, and J. P. Pinceaux, Phys. Rev. B **32**, 7611 (1985).

[6] W. B. Streett, Astron. J. **186**, 1107 (1986).

[7]J. A. Schouten, K. C. van den Bergh, and N. T. Trappeniers, J. Chem. Phys. **114**, 401 (1985).

[8]J. P. Pinceaux, J. P. Maury, and J. M. Besson, J. Phys. (Paris) Lett. **40**, L307 (1979).

[9]R. Le Toullec, J. P. Pinceaux, and P. Loubeyre (unpublished).

[10]R. A. Noack and W. B. Holzapfel, in *High Pressure Science and Technology,* edited by K. D. Timmerhaus and M. S. Barber (Plenum, New York, 1979), Vol. 1, p. G18.

[11]H. Dubost, in *Inert Gases,* Vol. 34 of *Springer Series in Chemical Physics,* edited by M. L. Klein (Springer-Verlag, Berlin, 1984), p. 145.

[12]W. B. Streett and A. L. Erickson, Phys. Earth. Plan. Int. **5**, 357 (1972).

[13]F. H. Ree, J. Phys. Chem. **87**, 2846 (1983).